Type Synthesis of Linkage-driven Self-adaptive Fingers

Lionel Birglen

Department of Mechanical Engineering, Ecole Polytechnique of Montreal,
Montreal, QC, H3T 1J4, Canada,
Tel: (514) 340-4711 #3329, Fax: (514) 340-5867,
lionel.birglen@polymtl.ca

Abstract

This paper aims at providing a method to synthesize mechanical architectures of self-adaptive robotic fingers driven by linkages. Self-adaptive mechanisms are used in robotic fingers to provide the latter with the ability to adjust themselves to the shape of the object seized without any dedicated electronics, sensor, or control. This type of mechanisms has been known for centuries but the increased capabilities of digital systems have kept them in the shadows. Recently, because of the lack of commercial and industrial success of complex robotic hands, self-adaptive mechanisms have attracted much more interest from the research community and several prototypes have been built. Nevertheless, only a handful of prototypes are currently known. It is the aim of this paper to present a methodology that is able to generate thousands of self-adaptive robotic fingers driven by linkages with two and three phalanges. First, potential kinematic architectures are synthesized using a well-known technique. Second, the issue of proper actuation and passive element(s) selection and location is addressed.

1 Introduction

Robotic hands are arguably the most popular end-effectors of robotic systems, at least within the research community. These devices have been developed with the aim of matching the human hand in terms of dexterity and adaptation capabilities, a difficult challenge with the current available technologies. Robotic hands are often designed to equip either a dextrous manipulator for pick-and-place tasks or a human being as a prosthetic device. Several pioneer prototypes have been developed, some of them for more than two decades, and include the Stanford/JPL hand [1], the Utah/MIT hand [2], and the hands from the DLR [3]. However, these prototypes have all been designed aiming at an anthropomorphic architecture where each joint is independently actuated. This correspondence between the joint and actuator axes leads to bulky hands and/or complicated power transmission devices. Furthermore, the complexity of controlling often more than twelve axes, simultaneously and in real-time, is especially demanding and yields significant costs. Hence, despite their capabilities, robotic hands have often little, if any, success outside research laboratories.

In the past few years, a significant increase in the development of innovative technologies for robotic hands has tried to address this lack of success. Significant efforts have been made to find designs simple enough to be easily built and controlled and a special emphasis has been placed on the reduction of the number of degrees of freedom (DOF), thereby decreasing the number of required actuators. A rapidly growing number of prototypes involve a smaller number of actuators without decreasing the number of DOF by taking advantages of self-adaptive mechanisms. These prototypes are either driven by tendons [4, 5, 6, 7] or linkages [8, 9, 10, 11, 12]. This approach leads to the automatic and mechanical adaptation of the robotic finger to the shape of the object seized. A well-known example of a self-adaptive two-DOF finger driven by linkages and its closing sequence are illustrated in Fig. 1. The finger is actuated through the lower link (cf. arrow) and a spring with a mechanical limit is used to maintain the finger fully extended. The closing sequence occurs with a continuous motion of the actuator. First, the finger behaves as a single rigid body in rotation about a fixed pivot. Second, the proximal phalanx makes contact with the object. Third, the actuation torque overcomes the preloading of the spring and the second phalanx is moved away from the mechanical limit and rotates with respect to the first phalanx. Finally, both phalanges are in contact with the object and the finger has completed the shape adaptation. The actuator force is distributed among the two phalanges in contact with the object [13].

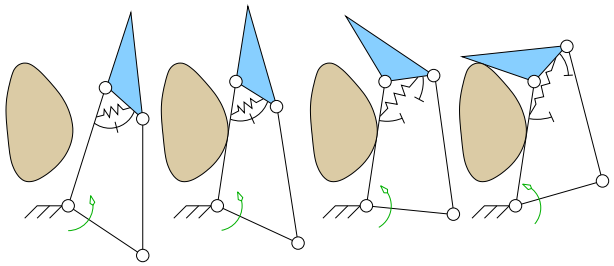

Fig. 1: Closing sequence of a two-DOF self-adaptive finger.

Self-adaptive mechanisms offer tremendous possibilities and have been known for decades. However, they have been kept in the shadows of the exponentially growing complex systems relying on digital architectures. Mechanical systems have been superseded by their electronic counterpart which provided better, more accurate, cheaper and faster means of performing computing tasks [14]. Nevertheless, the confinement of mechanical systems to the execution of motion/forces under the control of high-level controllers has to be considered as a design choice rather than an obligation. It is the primary

aim of this paper to present how to synthesize mechanisms that can be used to design highly efficient robotic hands which can adapt themselves to the shape of the object seized.

The properties required to achieve the self-adaptive behaviour are usually not detailed in the literature as they remain unclear. Only a few papers have been published dealing with theoretical aspects—i.e. valid not only for a single architecture but for a wide range of solutions—of self-adaptive mechanisms applied to grasping, namely [8, 11, 15, 13, 16]. Additionally, if the analysis of self-adaptive fingers is well detailed in the literature [17], to the best of the author's knowledge, only one reference [8] discusses the synthesis of such mechanisms. In the latter reference, two-phalanx self-adaptive fingers are synthesized and six architectures are obtained. However, as will be shown in this paper, this result is incomplete and using the same hypotheses, the actual number of possible architectures is 19 belonging to a much larger family of up to 1160 members. Extending the method, the synthesis of three-phalanx fingers is also addressed in this paper and the number of possible architectures of these fingers, even with a limited number of links is shown to be as large as 1864. Consequently, a method to properly select actuated joint(s) and the locations of the passive elements of the architectures, a required step to achieve the self-adaptation property, is presented.

2 Synthesis of Self-Adaptive Mechanisms for Robotic Fingers

2.1 Introduction

The self-adaptive behaviour of mechanical systems is obtained by combining two elements, namely a transmission linkage and passive elements. The main challenge faced when conceiving self-adaptive fingers is how to design the transmission linkage and what linkages do actually achieve this property? The answer to this latter question is surprisingly simple: *almost all linkages* can be used to design an acceptable transmission mechanism provided they satisfy a few simple hypotheses, namely:

1. the transmission linkage should reach the distal phalanx;
2. the transmission linkage should be connected to the ground;
3. the transmission linkage must not restrict the DOF of the finger.

The first two hypotheses are actually not even mandatory when designing robotic fingers with self-adaptation but restrict the present analysis to the self-adaptive part of the finger. Based on these two hypotheses, it follows that the system constituted by the finger and the transmission linkage is a closed-loop mechanism. Finally, the last hypothesis ensures that the mobility of the finger is not constrained by the transmission linkage, which would result in a coupled motion finger, losing the self-adaptation property. Based on these hypotheses a simple number synthesis, a method found in most textbook on the design of machinery, can be used generate all the possible mechanisms.

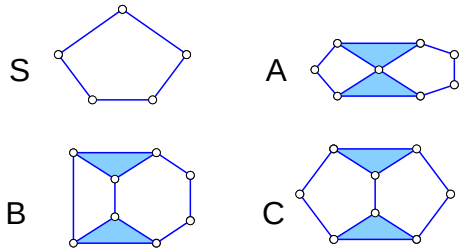

Fig. 2: Two-DOF closed-loop mechanisms with revolute joints.

2.2 Two-Phalanx Fingers

Two-phalanx fingers are defined by a serial planar architecture with three successive links—namely the ground, proximal and distal phalanges—connected with revolute joints. This architecture has two DOF. Therefore, one shall proceed with the number synthesis of two-DOF closed-loop mechanism. Let us assume that only binary and ternary links are considered for the sake of simplicity. One has

$$\begin{cases} L = B + T \\ L - 5 = T \end{cases} \tag{1}$$

where L is the number of links of the architecture, B is the number of binary links, and T is the number of ternary links. Please note that since the number of DOF is even, L must be odd. This set of equations has to be satisfied to obtain the compatible combinations of links with two-DOF. However, this synthesis method might miss some particular architectures with peculiar geometric relationships (e.g. the Bennett linkage or Hobermann spheres) which are not considered in this paper. If $L = 2k + 1$ with $k \geq 2$, one obtains:

$$\begin{cases} T = 2(k-2) \\ B = 5 \end{cases} \quad \text{for } k \geq 2. \tag{2}$$

If the number of links is limited to a reasonable range, e.g. $L \leq 7$, and considering only revolute joints, one obtains the mechanisms illustrated in Fig. 2. The five-bar linkage ($L = 5$) is the simplest two-DOF closed-loop mechanism and constitutes a special class termed S. If $L = 7$ ($k = 3$), there are only three possible architectures—termed A, B, and C—since there is only a finite number of possible connections between the ternary links while preserving the number of DOF.

Each one of these mechanisms can be used to design a two-phalanx robotic finger. The ground and proximal/distal phalanges must be chosen as three consecutive links of the previously obtained mechanisms, reflecting the serial architecture of robotic fingers. However, this choice is not entirely arbitrary as it must satisfy the hypotheses enunciated in Section 2.1. For instance, the finger can not be chosen as three links of the four-bar loops of mechanisms A or B for this choice would reduce the number of DOF of the finger to one. Removing symmetrical combinations, one obtains the architectures of linkage-driven robotic fingers illustrated in Fig. 3. Each combination is designated with a number corresponding to the choice of which link is the

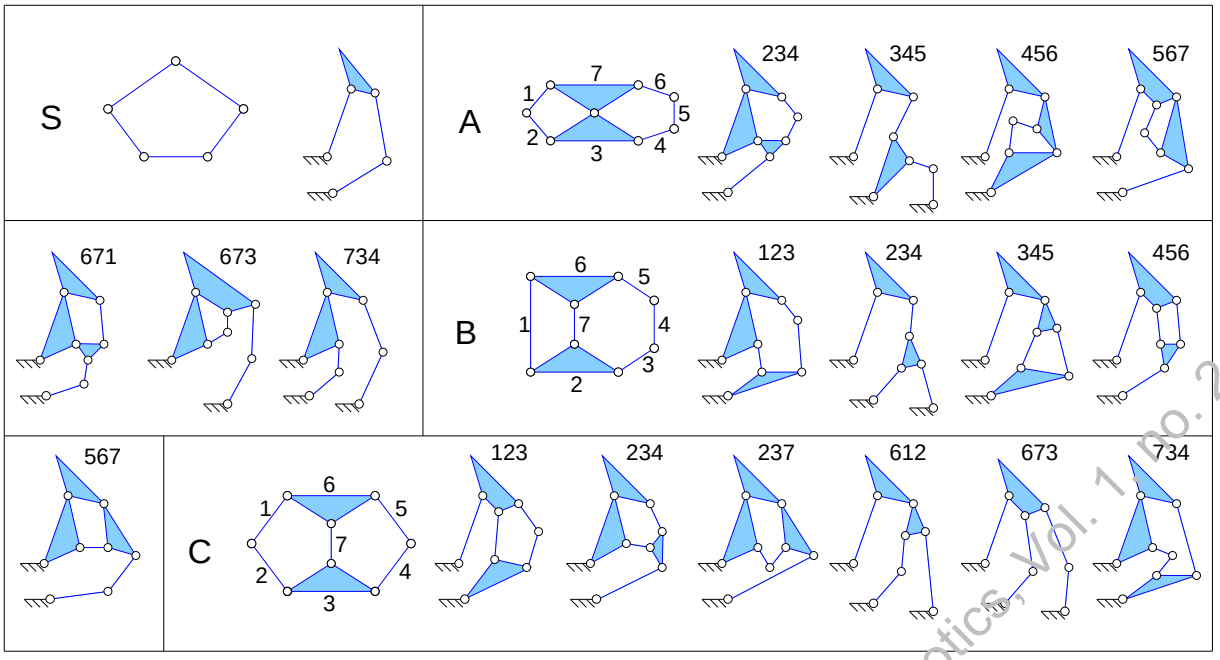

Fig. 3: Architectures of two-phalanx fingers with only revolute joints.

ground, proximal and distal phalanges (in this order) with respect to the nomenclature indicated in the figure. Each possible combination of ground/proximal/distal links are tried with the four classes of mechanisms. The combinations not satisfying the hypotheses of Section 2.1 are eliminated leaving 19 possible architectures of two-phalanx fingers with seven or less links connected with revolute joints. This number should be compared with the six architectures found in [8].

It should be noted that any joint of the transmission linkage can be replaced with a prismatic joint of arbitrary axis or more generally, any one-DOF joint (e.g. gears, cams, etc.). Considering that each joint can be either of the revolute or prismatic type and there are three joints in the transmission linkage of the class S, this class actually comprises up to eight mechanisms, illustrated in Fig. 4. However, since geometric constraints are not taking into account, not all of these linkages are acceptable and further investigations might be required if several prismatic joints are used. For instance, the last candidate of the class S illustrated in Fig. 4 comprising three prismatic joints in the transmission linkage is invalid. Indeed, the latter is kinematically redundant and unable to accommodate any rotation of the distal phalanx. The linkage itself still has two-DOF but the mobilities of the driven system are constrained by the transmission linkage. Similarly, with the architectures using two prismatic joints, the axes of the latter should not be parallel. Hence, when using more than one prismatic joint, the resulting mechanism should be carefully analyzed using dedicated tools such as screw theory. This verification is mandatory but beyond the scope of this paper since focus is primarily put on architectures with revolute joints. Nevertheless, this important point must be noted. Similarly, each one of the architectures belonging to the A, B and C classes illustrated in Fig. 3 is but the revolute-only member of a family comprising a maximal number of $2^6 = 64$ mechanisms if prismatic joints are considered. Therefore, the maximal possible number of architectures of two-phalanx fingers driven with linkages and revolute or prismatic joints is $1 \times 3 + 18 \times 64 = 1160$.

It should be emphasized that, in this section, the architectures are not referred to as self-adaptive or underactuated. Indeed, these designs can be fully actuated and are not necessarily self-adaptive. To obtain self-adaptive fingers, a number of actuators inferior to the number of DOF of the mechanism should be placed in coordination with passive elements. This issue is discussed in Section 3.

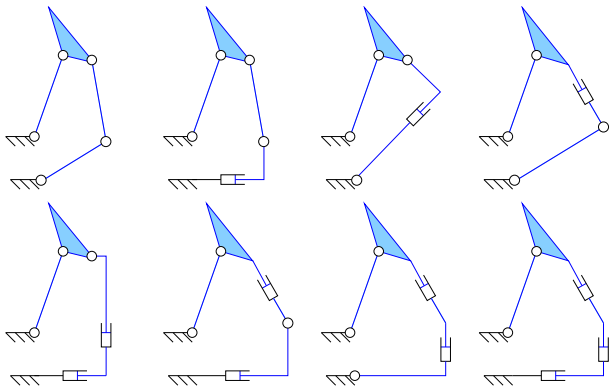

Fig. 4: Candidates of the class S of two-phalanx fingers.

2.3 Three-Phalanx Fingers

Similarly to Section 2.2, a number synthesis is used to generate all the possible candidate architectures of linkage-driven fingers with three-DOF. Assuming again that only binary and

ternary links are considered, one has

$$\begin{cases} L = B + T \\ L - 6 = T \end{cases}. \quad (3)$$

Since the number of DOF is odd, L must be even. This set of equations has again to be satisfied to obtain the compatible combinations of links with three-DOF. If $L = 2k$, one obtains:

$$\begin{cases} T = 2(k-3) \\ B = 6 \end{cases} \quad \text{for } k \geq 3. \quad (4)$$

If the number of links is limited to a reasonable range, e.g. $L \leq 8$, and with only revolute joints, one obtains six mechanisms. One of the latter is the six-bar linkage ($L = 6$) which is the simplest three-DOF closed-loop mechanism and constitutes a special class termed S. If $L = 8$, there are only five possible architectures, designated by letters from A to E.

Each one of these mechanisms can be used to design a three-phalanx self-adaptive finger. The ground and proximal/intermediate/distal phalanges must be chosen as four consecutive links of the previously obtained mechanisms. Again, this choice must satisfy the hypotheses enunciated in Section 2.1, for instance the finger cannot be chosen as four links of a four- or five-bar loop of mechanisms A, B, C or D for this choice would reduce the number of DOF of the finger to one or two. Similarly, any subchain of the finger cannot be chosen as three links of a four-bar linkage for the same reason. Removing symmetrical combinations, one obtains the fingers illustrated in Fig. 5. Each combination is designated with a number corresponding to the choice of which links are the ground, proximal, intermediate and distal phalanges (in this order) with respect to the nomenclature indicated in the figure. Therefore, there are 30 architectures of three-DOF robotic fingers satisfying the hypotheses of Section 2.1 with eight or less links and revolute joints. If prismatic joints in the transmission linkage are considered, this number grows to a maximal number of $1 \times 2^3 + 29 \times 2^6 = 1864$ possible architectures. Again, if prismatic joints are used, it should be verified that the mobility of the finger is not constrained by the transmission linkage.

2.4 Classification and Selection

Linkage-driven self-adaptive fingers found in the literature can be classified according to the nomenclature proposed in this paper, as illustrated in Table 1. Please note that, in this table, S refers to the two-phalanx special class proposed in Fig. 3. The three-phalanx special class is proposed in this paper for the first time to the best of the author's knowledge. The proposed nomenclature is established as follows: each architecture is identified to the class of closed-loop mechanism by the associated letter (A to E) followed by a sequence of 3 (with two phalanges) or 4 (with three phalanges) digits identifying the choice of links corresponding to the ground/phalanges arrangement. Therefore, with the exception of the trivial S class, no two- or three-phalanx architecture shares the same designation.

Table 1: Classification of self-adaptive fingers in the literature.

Label	Authors
$C234$	Itoh [18]
S, $B567$, $A671$, $B456$, $B345$, $C234$	Shimojima et al. [8]
S, $A671$, $B456$, $C234$ $A4567$, $B4567$	Laliberté and Gosselin [11, 19]
$C234$	Dubey and Crowder [20] (self-adaptive part of the finger)

Evidently, not all the architectures obtained with the synthesis method proposed in this section appears equally interesting. For instance, the fourbar loops of architectures $A567$ or $B345$ do not seem particularly useful, except maybe to relocate a position sensor. However, there is probably not a universal optimal architecture to design self-adaptive fingers. Past and current investigations by the author indicate that multistage architectures such as $A4567$ or $B4567$ usually have good performances with respect to the generated contact forces and size of the workspace. However, S-class fingers are by far the simplest architectures and therefore the least expensive to manufacture. Additionally, it is known by the author that they achieve good performances with respect to the contact forces. However, it is difficult to obtain a large workspace with a range of motion in the joints of the linkage comparable to multistage architecture (this is especially critical when dealing with compliant fingers). Furthermore, each architecture can obviously be optimized with respect to one or several criteria and it is very difficult (or maybe impossible) to predict which architecture will yield the "best optimum." Therefore, the designer might reduce the pool of candidates by inspection, optimize each of the considered architectures to obtain practical designs, and finally select the best design. However, this approach is not recommended since the elimination of candidate architectures might result in a poor selection if done by an unskilled designer. It is also important to note that for each architecture, one has to select the locations of the actuator(s) and passive elements and this choice will impact the performances of the design. This choice must not be made hastily as will be discussed in the next section.

3 Actuation and Passive Elements Location

3.1 Actuation

With each of the architectures obtained using the technique proposed in the previous sections, actuation and passive elements are required. Proper selection and location of both of them has to be dealt with carefully. Indeed, considering the architectures obtained in Figs. 3 and 5, one cannot arbitrarily select a joint in the finger to be actuated. This choice must be made in order for the actuation torque to be distributed to all the joints of the driven system (i.e. the joints between the phalanges). In this paper, focus is put on the case where a single actuator drives the mechanism. The actuation torque (or force in the case of a prismatic joint) distribution is a fundamental

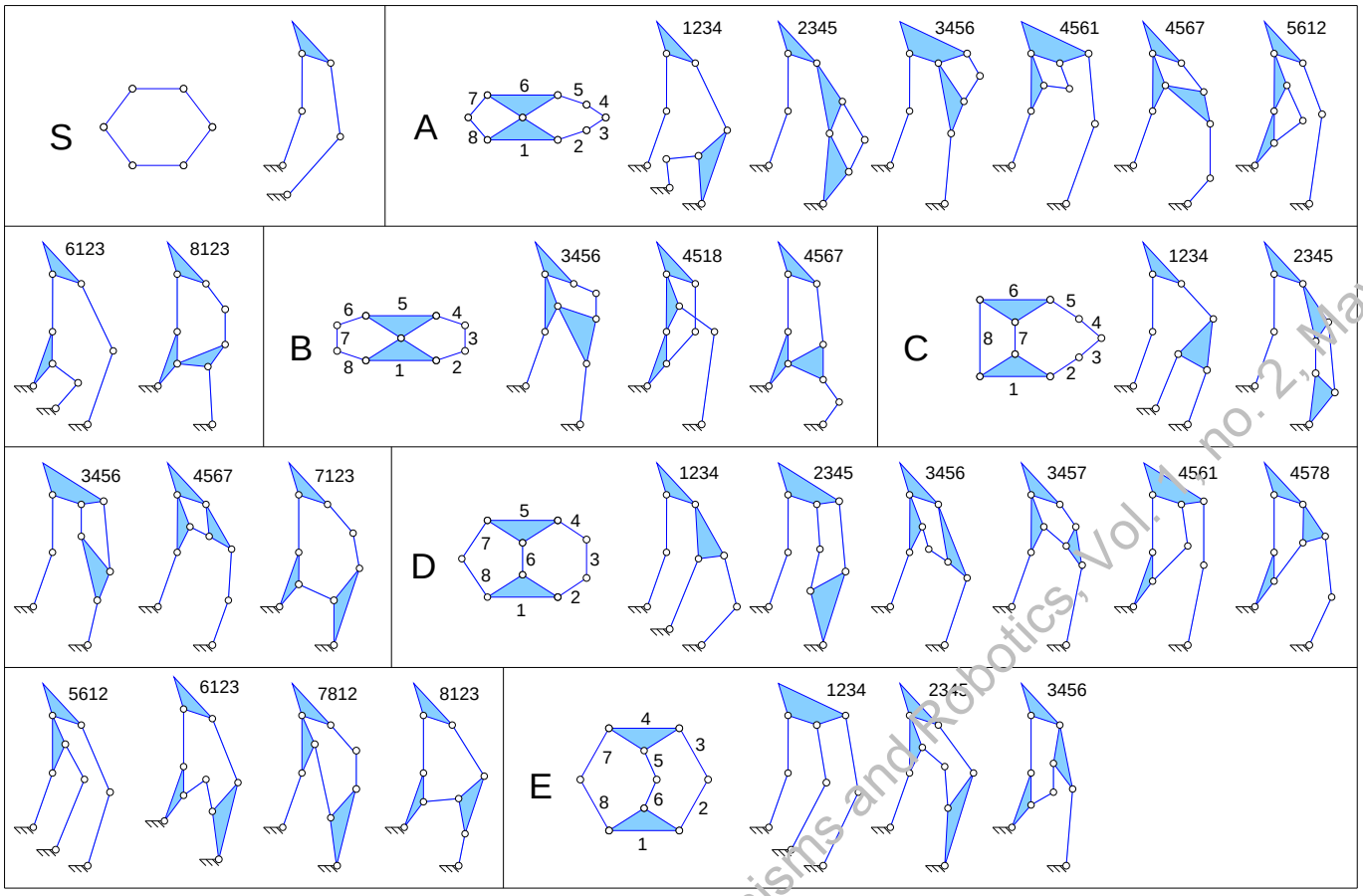

Fig. 5: Architectures of three-phalanx fingers with only revolute joints.

characteristic of self-adaptive fingers and an especially attractive design option if it avoids the burden of embedding several actuators in the finger. Several architectures proposed in Sections 2.2 and 2.3 might be actuated through a joint between the transmission linkage and the ground, but not all of them. The joint selected for actuation must satisfy the distribution condition, namely

$$\forall i \in [1, n],\ \exists \boldsymbol{\theta} \mid \frac{\partial \tau_i(\boldsymbol{\theta})}{\partial T_a} \neq 0 \tag{5}$$

where $\boldsymbol{\theta} = [\theta_1 \ \dots \ \theta_n]^T$ with respectively $n = 2$ and $n = 3$ for two- and three-phalanx fingers is the vector of the configuration states of the finger, i.e. the joint angles between the phalanges. Similarly, $\boldsymbol{\tau} = [\tau_1 \ \dots \ \tau_n]^T$ is the vector of the torques generated by the transmission linkage about these joints (cf. Fig. 6). Finally, T_a is the actuation torque. This distribution condition, despite its critical importance, usually does not clearly appear in the literature.

The relationship between the input and output torques can be established using either a static analysis or a virtual power approach. The distribution condition defined in eq. (5) physically means that for each joint of the driven finger there exists at least one configuration where the actuation torque is distributed to this joint. In other words, the joint torques of the driven finger must not be independent of the actuation torque. It should be noted that local particular configurations failing

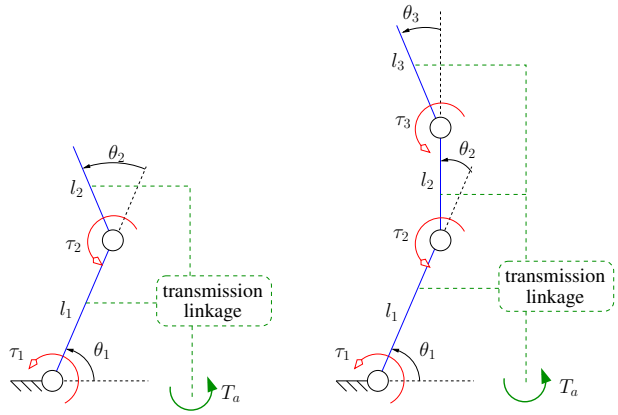

Fig. 6: Distribution of the actuation torque in two- and three-phalanx fingers.

this examination might exist, i.e. there often exists at least one joint i such as $\partial\tau_i/\partial T_a = 0$ for a specific value of $\boldsymbol{\theta}$. These local singular configurations should be avoided by design or located outside the workspace of the finger. Indeed, to ensure a closing motion of the phalanges, one must ensure that

$$\forall i \in [1, n], \quad \frac{\partial \tau_i(\boldsymbol{\theta})}{\partial T_a} > 0 \tag{6}$$

within the range of $\boldsymbol{\theta}$ corresponding to the workspace of the finger. It should be noted that τ_i with $i = 1, \dots, n$, namely

the joint torques of the driven finger, cannot be chosen for actuation because if the corresponding joint is locked by one or several external contacts, no torque distribution would occur.

To illustrate how the distribution condition can be used in locating the actuator of a self-adaptive finger, let us consider the architecture $A234$. With a simple static analysis one obtains

$$\begin{bmatrix} 0 \\ 0 \end{bmatrix} = \begin{bmatrix} 1 & 0 & A & B & C & D & E & F \\ 0 & 1 & 0 & 0 & 0 & G & H & I \end{bmatrix} \begin{bmatrix} \tau_1 \\ \tau_2 \\ \tau_3 \\ \tau_4 \\ \tau_5 \\ \tau_6 \\ \tau_7 \\ \tau_8 \end{bmatrix} \quad (7)$$

or

$$\mathbf{0} = \mathbf{S}_{A234}(\boldsymbol{\theta})\boldsymbol{\tau}^\star \quad (8)$$

where $\boldsymbol{\tau}^\star = [\boldsymbol{\tau}^T \tau_{n+1} \dots \tau_{n+m}]^T$ are the torques in the n joints of the driven finger and the m joints of the transmission linkage, as illustrated in Fig 7(a) with $n = 2$ and $m = 6$. The joints $n+1$ to $n+m$ are the candidates for actuation. The matrix $\mathbf{S}_{A234}$ is the Selection matrix of architecture $A234$ which allows to choose which joint can be actuated. The coefficients A through I are complex functions of the geometry of the mechanism and the angles θ_1 and θ_2. Despite their complexity, these coefficients can be obtained relatively effortless using a software package. According to eq. (7), the only valid choices of actuation locations with respect to the distribution condition are τ_6, τ_7 or τ_8. Indeed, as can be seen from the latter equation the torques in the driven finger can be written

$$\begin{aligned} -\tau_1 &= A\tau_3 + B\tau_4 + C\tau_5 + D\tau_6 + E\tau_7 + F\tau_8 \\ -\tau_2 &= G\tau_6 + H\tau_7 + I\tau_8. \end{aligned} \quad (9)$$

Hence τ_2 is independent of τ_6, τ_7 and τ_8 and if actuation is located in these locations, it will fail to satisfy the distribution condition. Usually with simple linkages like two-phalanx fingers, a skilled designer can readily identify unacceptable locations simply by inspection. However, if either more complicated driven systems are considered or a large number of links is used, the method presented in this section becomes mandatory. The relationship between the torques in joints of the driven finger and the transmission linkage can be established for any architecture obtained in Section 2. For instance, with the architecture termed "$Xijk$" one would obtain

$$\mathbf{0} = \mathbf{S}_{Xijk}(\boldsymbol{\theta})\boldsymbol{\tau}^\star \quad (10)$$

Not every architecture obtained using the methodology presented in Section 2 can pass the distribution condition. For instance, if one considers architecture $B4518$ illustrated in Fig. 7(b), one has

$$\mathbf{0} = \begin{bmatrix} 1 & 0 & 0 & A & B & C & 0 & 0 & 0 \\ 0 & 1 & 0 & D & E & F & G & H & I \\ 0 & 0 & 1 & 0 & 0 & 0 & J & K & L \end{bmatrix} \boldsymbol{\tau}^\star. \quad (11)$$

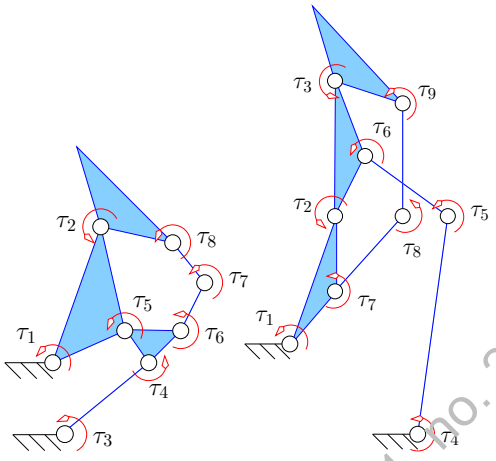

(a) $A234$ (b) $B4518$

Fig. 7: Actuation selection for architectures $A234$ and $B4518$.

Hence, no single joint of the transmission linkage can distribute its torque to all the joints of the finger. Therefore, to drive this architecture, at least two actuators are required. Nevertheless, even with two actuators, one can still preserve a self-adaptive behaviour since one DOF remains unconstrained. Requiring more than one actuator to ensure proper torque distribution is also fairly common if one considers quaternary (or pentagonal, etc.) links in the synthesis procedure while keeping a limited number of total links. The resulting mechanisms tend to have separate kinematic loops (e.g. Fig 8) preventing proper distribution of the actuation. This is the reason why they have not been considered in Section 2.

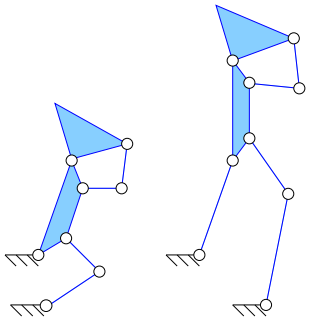

Fig. 8: Two- and three-phalanx finger architectures with a quaternary link.

3.2 Passive Elements

To drive a n-DOF system driven by a single actuator, $n-1$ supplementary DOF have to be constrained to obtain a statically determined system. Hence, a minimal number of $n-1$ passive elements are required. These elements have been referred to as "passive actuators" and although this is a contradiction in the terms, it is a fairly adequate description of their function. Since the objective is to apply an external constraint on the system, numerous elements can be used. The most common of these elements used in self-adaptive hands are illustrated in Fig. 9 and can be categorized into two families, namely triggered and continuous elements.

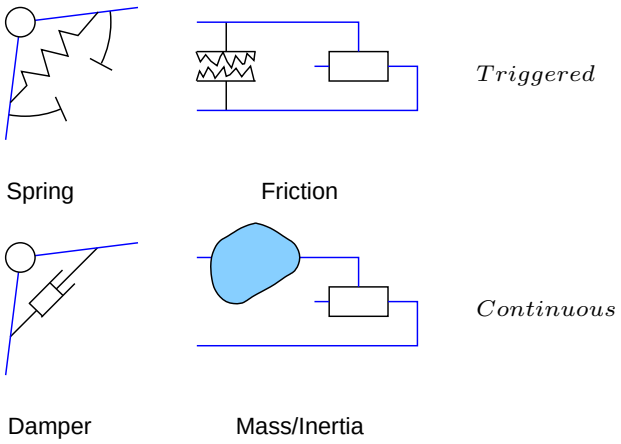

Fig. 9: Single joint passive elements.

Triggered elements allow motion in the joint only after a certain force or torque arises in the latter. The most common solutions to achieve this behaviour is the preloaded spring, e.g. in the MARS and SARAH hands [11], and the friction clutch, e.g. in the BarrettHand [21]. Continuous elements are also possible despite being far less popular. These elements exhibit a continuous motion of the associated joint with respect to the force or torque applied. Examples of continuous elements are the damper (a non-preloaded spring is also possible), and a mass or inertial element as illustrated in Fig. 9. It should be noted that passive, and especially continuous, elements can be combined (e.g. a spring in parallel with a damper). Triggered elements are used to temporarily decrease the number of DOF of the finger to match the number of actuators. Furthermore, they can be used to constrain the shape of the finger during the pregrasping phase if correctly located and preloaded. On the other hand, continuous elements have a similar effect on the finger as actuators and their effect must be distributed to the joints of the driven finger as discussed in the previous section. The location of passive elements, can be determined using a procedure similar to the one described in the previous section as will be detailed. However, in this case, placing a passive element in one of the joints of the finger is an acceptable choice. Actually, from an historical perspective, passive elements, continuous or not, have been consistently located in these joints in order to maintain the finger phalanges aligned during the pregrasping phase, as illustrated in Fig. 1. This is a valid choice leading to simpler expressions as will be shown. However, it is not at all mandatory. If more than one passive element is required, it should be noted that only their combined effect has to apply to the driven joints, not each element separately. This is the fundamental difference to be considered in the selection of an acceptable location between actuation and passive elements. For instance, with three-phalanx fingers, the first passive element can constrain the first two joints of the finger while the second element only applies a torque to the third joint.

The locations of the passive elements in the joints of an architecture obtained using the method presented in Section 2 must be chosen in order for the self-adaptive finger to be statically determined. This condition on the static equilibrium of the system is related to the Transmission matrix presented in [13] as will be presented in this section. The contact forces generated by the finger are related to the torques of the actuator and passive elements. Indeed, $\boldsymbol{\tau}$ can be expressed as

$$\boldsymbol{\tau} = \mathbf{J}^T \mathbf{f} \tag{12}$$

where $\mathbf{f}$ is the vector of the generated contact forces (one for each phalanx) and assumed normal to the surface of the phalanx. The matrix $\mathbf{J}$ is the Jacobian matrix of the grasp as proposed in [13]. This matrix should not be confused with the Grip Transform matrix [22], usually noted $\mathbf{G}$ and commonly found in the literature about grasping. The generated contact forces are related to the actuation and passive elements torques by

$$\mathbf{f} = \mathbf{J}^{-T} \mathbf{T}^T \mathbf{t} \tag{13}$$

where vector $\mathbf{t}$ contains the actuated and passive elements torques, i.e. $\mathbf{t} = [T_a \; T_2 \; \dots \; T_n]^T$ with $n = 2$ or 3, respectively with two- and three-phalanx fingers. The torques T_i are due to the passive elements, e.g. $T_i = -K_i \Delta\alpha_i$ if a simple rotational spring is considered (K_i and α_i are respectively the stiffness and deflection angle associated with this spring). The above equation is valid with any location of the passive elements since the matrix $\mathbf{T}$ has to be built consistently with the choice of these locations. This matrix $\mathbf{T}$ is the second form of the Transmission matrix proposed in [23] and characterizes the transmission linkage. It relates the velocities of the actuated and passive element joints to the velocities of the driven joints of the finger, namely

$$\boldsymbol{\omega} = \mathbf{T}\dot{\boldsymbol{\theta}} \tag{14}$$

with $\boldsymbol{\omega} = [\dot{\theta}_a \; \dot{\theta}_{p_1} \; \dots \; \dot{\theta}_{p_{n-1}}]^T$ where θ_a is the angle of the actuated joint (selected using the procedure described in Section 3.1) and θ_{p_i} are the angles of the selected joints corresponding to the passive elements. Considering eqs. (12) and (13), one readily obtains

$$\boldsymbol{\tau} = \mathbf{T}^T \mathbf{t}. \tag{15}$$

By comparing eqs. 10 and 15, it clearly appears that the Transmission and the Selection matrices are closely related. Indeed, the lines of the Transmission matrix are a subset of the columns of the Selection matrix corresponding to the joints actuated and with passive elements (with a difference of sign). Indeed, eq. (15) can be written

$$\mathbf{0} = \begin{bmatrix} \mathbf{1}_n & -\mathbf{T}^T \end{bmatrix} \begin{bmatrix} \boldsymbol{\tau} \\ \mathbf{t} \end{bmatrix} \tag{16}$$

where $\mathbf{1}_n$ is the $n \times n$ identity matrix. By definition of vector $\mathbf{t}$, the first line of the Transmission matrix corresponds to the actuated joint and the subsequent lines to the passive elements.

According to eq. (15), the relationship between the torques in the driven joints and in the actuated/passive joints is linear. Considering this linear relationship, to obtain a statically

determined mechanism one must chose the location of the passive elements such that

$$\ker(\mathbf{T}) = \mathbf{0} \quad \text{or} \quad \det(\mathbf{T}) \neq 0. \tag{17}$$

Therefore, the second step in the synthesis procedure as proposed in this paper, after the mechanical architecture of the finger has been chosen, is to construct a Transmission matrix $\mathbf{T}$ from the Selection matrix such as:

1. no element on its first line is always zero (distribution condition of the actuation),
2. the matrix (generally) has full rank.

Usually, several choices of locations for the passive elements satisfy the latter condition. Certain locations such as the joints between the phalanges are typically preferred by the designer as they lead to specific pregrasping kinematic behavior of the finger as will discussed in the next section.

Finally, as a brief summary before the examples, the contributions of this paper include:

- thousands of novel architectures of self-adaptive robotic fingers,
- the method to generate the latter,
- the introduction of a Selection matrix to choose the locations of actuation and passive elements,
- the methodology to make this choice based on the rank of the resulting Transmission matrix and the distribution condition.

3.3 Examples

Comparison of two-phalanx architectures

The tools presented in this paper can be used to compare the different architectures of two-phalanx fingers obtained in Section 2.2. As an example, let us suppose that one want to select an architecture among the latter to design a self-adaptive fingers. It is assumed that only revolute joints are acceptable and that the designer desires a transmission linkage with only one attachment to the ground. Due to the latter hypothesis, the architectures $A345$, $A734$, $B234$, $C612$ and $C673$ are eliminated leaving 14 valid choices. With the geometric parameters presented in Fig. 10 where the torque nomenclature in the transmission linkage is detailed, the expressions of the corresponding Selection matrices are presented in Table 2. Again, due to the complexity of the symbolic expressions of these matrices, only numerical results (rounded to one digit) are presented with the geometric parameters and configurations corresponding to Fig. 10. To fit within the limited width of this page, the first two columns of each Selection matrix—i.e., the identity matrix of dimension two—has been omitted.

To evaluate the remaining architectures, it is assumed that the finger must be actuated through the link attached to the ground. Hence, the first line of the transmission matrix correspond to the third (by convention) column of the Selection matrix. From this constraint, the architecture $A234$ and $B123$ are eliminated since one element of the third column of their associated Selection matrix is zero. It can be verified that this is true for any geometric configuration of the finger. Therefore, the distribution condition is not satisfied for these architectures and locations of actuation. Interestingly, the first element on the second line of matrix $\mathbf{S}_{B345}$ is also zero (actually it is very small—approx. 0.02—but not *exactly* zero) which similarly eliminates this architecture. It can be verified though by using another geometric configuration that this situation is only local with architecture $B345$. Now, one needs a performance index to compare the fingers. In this example, the uniformity of the torques in the driven joints is chosen. The associated index can be defined as

$$I = \frac{\tau_1}{\tau_2}\delta(\boldsymbol{\tau}) \tag{18}$$

where 1 is the ideal case and $\delta(\boldsymbol{\tau})$ is a Kronecker-like symbol for the positiveness of vector $\boldsymbol{\tau}$ that allows to discard situations where both torques are negative (although this situation is not critical if actuation is reversible):

$$\delta(\boldsymbol{\tau}) = \begin{cases} 1 \text{ if } \tau_i > 0,\ \forall\, i \\ 0 \text{ otherwise} \end{cases} \tag{19}$$

If the spring torque is small and considered negligible with respect to the actuation torque this index can be very simply

Table 2: Non-trivial columns of the Selection matrices.

S	$\begin{bmatrix} 1.1 & -0.7 & 0.5 \\ 0.4 & -0.6 & 1.2 \end{bmatrix}$
$A234$	$\begin{bmatrix} 0.7 & 1.3 & 1.6 & 3.0 & -3.2 & 1.7 \\ 0 & 0 & 0 & 0.9 & -2.4 & 2.5 \end{bmatrix}$
$A456$	$\begin{bmatrix} 1.0 & 0.6 & 0.6 & -0.3 & 0.9 & -1.1 \\ 0.5 & 0.9 & 1.5 & -0.5 & 1.3 & -1.7 \end{bmatrix}$
$A567$	$\begin{bmatrix} 1.0 & -0.5 & -0.5 & 0.3 & -0.7 & 0.9 \\ 0.5 & -0.8 & -1.3 & 0.9 & -1.8 & 2.2 \end{bmatrix}$
$A671$	$\begin{bmatrix} 1.4 & 2.0 & 1.6 & 0 & 0 & 0 \\ 0.6 & 1.5 & 2.2 & 1.2 & 1.4 & 1.2 \end{bmatrix}$
$A673$	$\begin{bmatrix} 2.4 & -3.0 & 1.3 & -0.3 & -1.0 & 1.0 \\ 2.0 & -3.9 & 2.9 & 1.0 & 2.7 & -2.8 \end{bmatrix}$
$B123$	$\begin{bmatrix} -1.0 & -1.3 & -1.3 & -0.6 & -0.4 & 0.2 \\ 0 & 0 & 0 & 0.7 & 2.9 & 3.2 \end{bmatrix}$
$B345$	$\begin{bmatrix} 0.7 & 2 & -6.6 & 4.5 & -3.5 & -7.7 \\ 0.0 & 4.0 & -11.1 & 8.1 & -5.9 & -13.0 \end{bmatrix}$
$B456$	$\begin{bmatrix} 1.0 & 0.1 & 0.9 & 0.8 & 1.1 & 1.0 \\ 0.2 & 1.1 & 2.3 & 2.0 & 2.8 & 2.5 \end{bmatrix}$
$B567$	$\begin{bmatrix} 1.5 & 1.4 & -0.9 & 0 & 0 & 0 \\ 0.5 & 0.5 & 0.1 & 1.1 & 1.5 & 1.3 \end{bmatrix}$
$C123$	$\begin{bmatrix} 1.5 & 1.9 & 1.3 & 0.2 & 1.6 & 1.2 \\ 0.8 & 1.7 & 0.6 & 1.2 & 1.7 & 2.0 \end{bmatrix}$
$C234$	$\begin{bmatrix} 1.2 & 2.3 & 3.3 & -1.2 & 3.5 & 1.4 \\ 0.6 & 1.7 & 1.7 & 0.5 & 3.4 & 2.2 \end{bmatrix}$
$C237$	$\begin{bmatrix} 0.8 & 0.4 & -9.9 & 0.9 & 1.1 & -0.8 \\ 0.2 & 0.7 & -1.4 & 1.8 & 0.5 & 0.9 \end{bmatrix}$
$C734$	$\begin{bmatrix} 1.0 & 0.4 & 0.4 & 1.2 & 0 & 1.3 \\ 0.4 & 0.6 & 1.2 & 1.0 & 0.8 & 0.3 \end{bmatrix}$

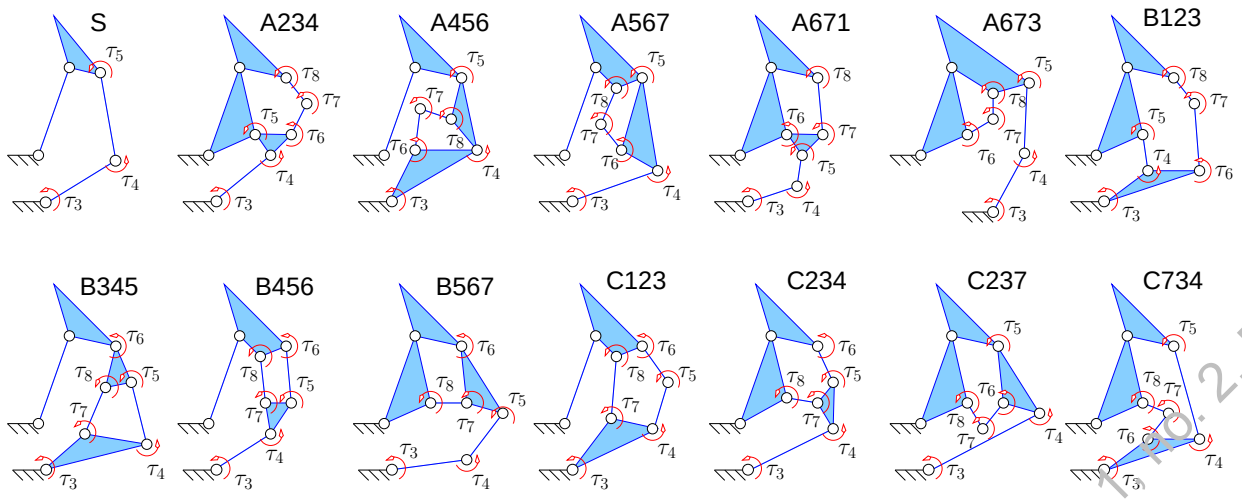

Fig. 10: Torque nomenclature of the candidate two-phalanx fingers.

expressed for each architecture as the ratio between the elements of the third column of its Selection matrix. Note that the performance measured by this index is not the uniformity of the contact forces (also referred to as force isotropy [17]) which might be more interesting practically but involves the Jacobian matrix of the grasp. The numerical values of the performance index for each architectures considered are presented in Table 3.

Table 3: Performance index I for the considered architectures.

S	$A456$	$A567$	$A671$	$A673$	$B456$
2.7	2	2	2.3	1.2	5
$B567$	$C123$	$C234$	$C237$	$C734$	
3	1.9	2	4	2.5	

From these results it can be seen that the best architecture is $A673$ and considering its Selection matrix, the required spring can be placed in any of the other joints of the finger. Taking into account the performance index previously defined in eq. (18) this element has the least impact on the performance index when located in the joint corresponding to τ_6.

As seen in this example, the Selection matrix can be used to select to compare architectures of self-adaptive fingers and also select a location for passive elements. Although, it should be said that this example is only presented for illustration purposes and to be fair, the geometric parameters of each architecture should have been optimized with respect to the performance index before comparing them.

Selection of actuation location

The methodology developed in this paper can also be used to choose optimal location for actuation with a particular design of self-adaptive finger. As an example, let us consider the architecture $A2345$ illustrated in Fig. 11. Obtained using a simple static analysis, the Selection matrix of this architecture is:

$$\mathbf{S}_{A2345} = \begin{bmatrix} \mathbf{u}_1 & \mathbf{u}_2 & \mathbf{u}_3 & \mathbf{v}_1 & \mathbf{v}_2 & \mathbf{v}_3 & \mathbf{v}_4 & \mathbf{v}_5 & \mathbf{v}_6 \end{bmatrix} = \begin{bmatrix} 1 & 0 & 0 & A & B & C & D & E & F \\ 0 & 1 & 0 & G & H & I & J & K & L \\ 0 & 0 & 1 & M & N & O & P & Q & R \end{bmatrix}. \quad (20)$$

The expressions of the coefficients A to R are obtained relatively effortless but span several pages and are therefore not presented here due to lack of space. From eq. (20), it appears that any of the six joints in the transmission linkage can be selected for actuation (cf. Section 3.1). However, to select the locations of the two required passive elements, attention should be paid to the rank of the matrices created from combining columns of the Selection matrix. In particular, one should notice that the fifth and last three columns of $\mathbf{S}_{A2345}$ are linearly dependent, namely one has

$$\text{rank} \begin{bmatrix} \mathbf{v}_2 & \mathbf{v}_4 & \mathbf{v}_5 & \mathbf{v}_6 \end{bmatrix} = 1. \quad (21)$$

This linear dependency usually does not clearly appear if a software package is used to obtain the Selection matrix but can nevertheless be verified numerically. The reduced rank of eq. (21) is characteristic of a one-DOF closed-loop in the transmission mechanism. For instance, if the values of the geometric parameters are chosen to correspond to Fig. 11, the numerical value of $\mathbf{S}_{A2345}$ is

$$\begin{bmatrix} 1 & 0 & 0 & -3.4 & 5.9 & -3.5 & 2.2 & 1.2 & 2.5 \\ 0 & 1 & 0 & -1.9 & 3.5 & -2.5 & 1.3 & 0.7 & 1.4 \\ 0 & 0 & 1 & -1.4 & 3.1 & -2.8 & 1.2 & 0.6 & 1.3 \end{bmatrix}. \quad (22)$$

The reduced row echelon form of the matrix formed by the last six columns of the previous numerical example is

$$\begin{bmatrix} 1 & 0 & 0 & 0 & 0 & 0 \\ 0 & 1 & 0 & 0.38 & 0.20 & 0.42 \\ 0 & 0 & 1 & 0 & 0 & 0 \end{bmatrix}. \quad (23)$$

where it clearly appears that each pair of the columns corresponding to $\mathbf{v}_2$, $\mathbf{v}_4$, $\mathbf{v}_5$, and $\mathbf{v}_6$ is linearly dependent, at least

locally. Thus, only one of the corresponding joints can be used to place either actuation or a passive element. If two of more of these joints are used, the Transmission matrix will loose rank and become singular in all configurations. Again, in this very simple example, this result could be readily found by inspection noting the closed-loop in the linkage.

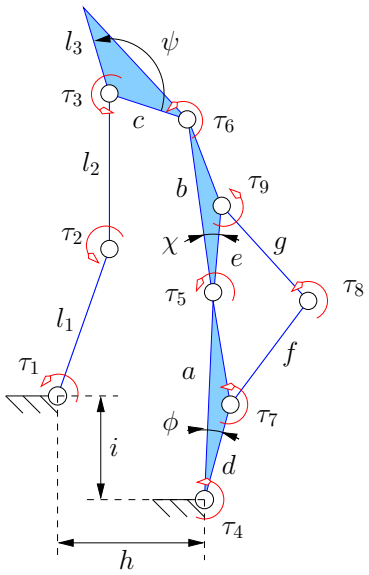

Fig. 11: Parameters of architecture $A2345$.

Subsequently, one has to choose the locations of the passive elements. The latter can be located in any joints of the mechanism distinct from the one selected for actuation, providing that the resulting Transmission has generally full rank (cf. Section 3.2). Let us assume that these locations are chosen by a kinematic constraint, e.g. it is desired that during the pregrasping phase all the phalanges stay aligned in order to increase the reachability of the finger. This is very common in the designs of self-adaptive fingers but it is important to note that this choice is absolutely not mandatory: passive elements can be located in any joints satisfying the rank condition of the Transmission matrix.

From this kinematic constraint, both passive elements are required to be springs located between the phalanges (proximal-intermediate and intermediate-distal joints). It is trivial to demonstrate from eq. (20) that these locations allow for a full rank Transmission matrix for any location of the actuated joint. Finally, deciding the location of the actuator in one of the six possible locations is not a trivial task, each location is a valid choice. Indices can be used to evaluate the performance of each possible choice. For instance, a measure can be obtained on how far one is to losing contact with one phalanx by including a "distance" from the vanishing of the smallest component of the contact forces as proposed in [13]. This index is noted η and using the geometric parameters listed in Table 4, its value is computed over a workspace defined by $\pi/4 < \theta_1 < 3\pi/4$ and $0 < \theta_i < \pi/2$ for $i = 2, 3$. This set of geometric parameters has been rapidly chosen to allow the finger to reach the entire workspace. The results are presented in Table 5 (the contacts are assumed at mid-phalanx).

Table 4: Geometric parameters.

l_1	l_2	l_3	ψ	a	b	c	d
1	0.7	0.5	$\pi/2$	2	2.5	0.2	1
e	f	g	h	i	ϕ	χ	
1	1	1	0.2	0	0	0	

Table 5: Index η for different locations of the actuation

Actuation ($T_a =$)	τ_4	τ_5	τ_6	τ_6	τ_8	τ_9
η (10^{-5})	7.4	0.012	0	0.003	0.013	0.004

Hence, for this geometry of the finger the optimal location for the actuator by far is in τ_4. It is intriguing that this location also permits attaching the actuator to the ground and therefore, might have been the preferred choice from a practical design point of view. However, this result does not necessarily hold with a different set of geometric parameters and/or with other architectures of fingers. Furthermore, similarly to the previous example, the geometric parameters of the finger are design variables that should also be optimized for each location of the actuator to yield a fair comparison. Again, this is beyond the scope of this example.

4 Conclusions

This paper has presented a method to synthesize self-adaptive robotic fingers using linkages. First, closed-loop mechanical architectures were generated using a number synthesis in which and phalanges were chosen as a set of consecutive links whose mobility is not restrained. Consequently, selection of the location of the actuated joint is addressed based on the distribution condition. This condition is maybe *the* fundamental property required with self-adaptive mechanisms for grasping and is presented here for the first time. The selection of the location(s) of passive element(s) completes the analysis. The selection of a proper set of joints where these passive elements can be placed is shown to be equivalent to finding a full-rank Transmission matrix. It is the main intention of this paper to provide tools to design innovative architectures of self-adaptive fingers. Common confusions or even mistakes (also done by the author himself) must be dissipated. Self-adaptive mechanisms can have a wide range of applications and offer tremendous potential capabilities. It is the opinion of the author that future mechatronic and robotic systems can greatly benefit from self-adaptation, not in replacement of electronics and control but completed by them. Innovative mechanical designs and the kinematics of these systems must be carefully studied. Indeed, kinematics is the essence of self-adaptive mechanisms.

Acknowledgments

The financial support of Natural Sciences and Engineering Research of Canada (NSERC) is acknowledged. The author wishes to express his gratitude to Louis-Alain Larouche for his help in obtaining the numerical values of the first example in Section 3.3.

References

[1] Salisbury, J. K. and Craig, J. J., "Articulated Hands: Force Control and Kinematic Issues," *The International Journal of Robotics Research*, Vol. 1, No. 1, pp. 4–17, 1982.

[2] Jacobsen, S. C., Iversen, E. K., Knutti, D. F., Johnson, R. T., and Biggers, K. B., "Design of the Utah/MIT Dextrous Hand," *Proceedings of the 1986 IEEE International Conference on Robotics and Automation*, pp. 1520–1532, San Francisco, CA, USA, April, 1986.

[3] Butterfass, J., Grebenstein, M., Liu, H., and Hirzinger, G., "DLR-Hand II: Next Generation of a Dextrous Robot Hand," *Proceedings of the 2001 IEEE International Conference on Robotics and Automation*, pp. 109–114, Seoul, Korea, May 21-26, 2001.

[4] Hirose, S. and Umetani, Y., "The Development of Soft Gripper for the Versatile Robot Hand," *Mechanism and Machine Theory*, Vol. 13, pp. 351–358, 1978.

[5] Crisman, J. D., Kanojia, C., and Zeid, I., "Graspar: A Flexible, Easily Controllable Robotic Hand," *IEEE Robotics and Automation Magazine*, pp. 32–38, June, 1996.

[6] Massa, B., Roccella, S., Carrozza, M. C., and Dario, P., "Design and Development of an Underactuated Prosthetic Hand," *Proceedings of the 2002 IEEE International Conference on Robotics and Automation*, pp. 3374–3379, Washington, DC, USA, May, 2002.

[7] Higashimori, M., Kaneko, M., Namiki, A., and Ishikawa, M., "Design of the 100G Capturing Robot Based on Dynamic Preshaping," *International Journal of Robotics Research*, Vol. 24, No. 9, pp. 743–753, September, 2005.

[8] Shimojima, H., Yamamoto, K., and Kawakita, K., "A Study of Grippers with Multiple Degrees of Mobility," *JSME International Journal*, Vol. 30, No. 261, pp. 515–522, 1987.

[9] Bekey, G. A., Tomovic, R., and Zeljkovic, I., *Control Architecture for the Belgrade/USC Hand in Dextrous Robot Hands*, Springer-Verlag, New-York, 1999.

[10] Ulrich, N. T., *Methods and Apparatus for Mechanically Intelligent Grasping*, US Patent No. 4 957 320, 1988.

[11] Laliberté, T. and Gosselin, C., "Simulation and Design of Underactuated Mechanical Hands," *Mechanism and Machine Theory*, Vol. 33, No. 1/2, pp. 39–57, 1998.

[12] Kennedy, B., "Three-Fingered Robot Hand With Self-Adjusting Grip," *Nasa Tech Briefs*, Vol. 25, No. 12, pp. 59, December, 2001.

[13] Birglen, L. and Gosselin, C., "Kinetostatic Analysis of Underactuated Fingers," *IEEE Transactions on Robotics and Automation*, Vol. 20, No. 2, pp. 211–221, April, 2004.

[14] Gosselin, C., "Adaptive Robotic Mechanical Systems: A Design Paradigm," *ASME Journal of Mechanical Design*, Vol. 128, No. 1, pp. 192–198, January, 2006.

[15] Hirose, S., "Connected Differential Mechanism and its Applications," *Proceedings of 1985 International Conference on Advanced Robotics*, pp. 319–325, Tokyo, Japan, September, 1985.

[16] Birglen, L. and Gosselin, C., "Grasp-State Plane Analysis of Two-Phalanx Underactuated Fingers," *Mechanism and Machine Theory*, Vol. 41, No. 7, pp. 807–822, 2006.

[17] Birglen, L., Laliberté, T., and Gosselin, C., *Underactuated Robotic Hands*, Springer, 2008, ISBN 9783540774587.

[18] Itoh, H., *Mechanical Hand*, US Patent No. 3 927 424, 1975.

[19] Gosselin, C. and Laliberté, T., *Underactuated mechanical finger with return actuation*, US Patent No. 5 762 390, 1996.

[20] Dubey, V. N. and Crowder, R. M., "A Finger Mechanism For Adaptive End Effectors," *Proceedings of 2002 ASME Design Engineering Technical Conferences*, Montreal, Canada, September 29-October 2, 2002.

[21] Ulrich, N. T., *Grasping with Mechanical Intelligence*, Ph.D. Thesis, School of Engineering and Applied Sciences, University of Pennsylvania, Philadelphia, Pennsylvania, December, 1988.

[22] Mason, M. T. and Salisbury, J. K., *Robot Hands and the Mechanics of Manipulation*, The MIT Press, 1985.

[23] Birglen, L., *Analysis and Control of Underactuated Robotic Hands*, Ph.D. Thesis, Faculté des sciences et de génie, Université Laval, Québec, Canada, October, 2004.